Looking for a varying α in the cosmic microwave background

P. P. Avelino,[1,2,*] C. J. A. P. Martins,[3,1,†] G. Rocha,[1,4,‡] and P. Viana[1,5,§]
[1] *Centro de Astrofísica, Universidade do Porto, Rua das Estrelas s/n, 4150-762 Porto, Portugal*
[2]*Departamento de Física da Faculdade de Ciências da Universidade do Porto, Rua do Campo Alegre 687, 4169-007 Porto, Portugal*
[3]*Department of Applied Mathematics and Theoretical Physics, Centre for Mathematical Sciences, University of Cambridge, Wilberforce Road, Cambridge CB3 0WA, United Kingdom*
[4]*Department of Physics, University of Oxford, Nuclear & Astrophysics Laboratory, Keble Road, Oxford OX1 3RH, United Kingdom*
[5]*Departamento de Matemática Aplicada da Faculdade de Ciências da Universidade do Porto, Rua das Taipas 135, 4050 Porto, Portugal*
(Received 29 August 2000; published 21 November 2000)

We perform a likelihood analysis of the recently released BOOMERanG and MAXIMA data, allowing for the possibility of a time-varying fine-structure constant. We find that in general these data prefer a value of α that was smaller in the past (which is in agreement with measurements of α from quasar observations). However, there are some interesting degeneracies in the problem which imply that strong statements about α cannot be made using this method until independent accurate determinations of $\Omega_b h^2$ and H_0 are available. We also show that a preferred lower value of α comes mainly from the data points around the first Doppler peak, whereas the main effect of the high-l data points is to increase the preferred value for $\Omega_b h^2$ (while also tightening the constraints on Ω_0 and H_0). We comment on some implications of our results.

PACS number(s): 98.80.Cq, 04.50.+h, 95.35.+d, 98.70.Vc

I. INTRODUCTION

There has been a recent growth of interest in theories where some of the usual constants of nature are actually time- and/or space-varying quantities. Most notably, the possibility of a time-varying fine-structure α has been the subject of a considerable amount of work, both at the theoretical and experimental or observational level.

From the theoretical point of view, the motivation comes from the recent work on higher-dimensional theories [1], which are thought to be required to provide a consistent unification of the known fundamental interactions. In such theories the ‘‘effective’’ three-dimensional constants are typically related to the ‘‘true’’ higher-dimensional constants via the radii of the (compact) extra dimensions [2]. On the other hand, these radii often have a nontrivial evolution, naturally leading to the expectation of time (or even space) variations of the ‘‘effective’’ coupling constants we can measure [3–5].

There are a number of different ways in which a variation of α can be modeled. From a ‘‘theoretical’’ point of view, the more convenient one appears to be to interpret it as a variation in the speed of light c [6–9], but other alternatives have been explored [10]. It is also possible to analyze the consequences of the variation of α in a more phenomenological context, as was done in [11,12].

On the observational level, the situation is at present somewhat confusing—see [13] for a brief summary. The best limit from laboratory experiments (using atomic clocks) is [14]

$$|\dot{\alpha}/\alpha| < 3.7\times 10^{-14}\ \text{yr}^{-1}. \tag{1}$$

Measurements of isotope ratios in the Oklo natural reactor provide the strongest geophysical constraints [15],

$$|\dot{\alpha}/\alpha| < 0.7\times 10^{-16}\ \text{yr}^{-1}, \tag{2}$$

although there are suggestions [16] that due to a number of nuclear physics uncertainties and model dependencies a more realistic bound is $|\dot{\alpha}/\alpha| < 5\times 10^{-15}$ yr^{-1}. Note that these measurements effectively probe timescales corresponding to a cosmological redshift of about $z\sim 0.1$ (compare with astrophysical measurements below).

Three kinds of astrophysical tests have been used. First, big bang nucleosynthesis [17] can in principle provide rather strong constraints at very high redshifts, but it has a strong drawback in that one is always forced to make an assumption on how the neutron to proton mass difference depends on α. This is needed to estimate the effect of a varying α on the ^{4}He abundance. The abundances of the other light elements depend much less strongly on this assumption, but on the other hand these abundances are much less well known observationally. Hence one can only find the relatively weak bound

$$|\Delta\alpha/\alpha| < 2\times 10^{-2}, \quad z\sim 10^{9}\text{–}10^{10}. \tag{3}$$

Secondly, observations of the fine splitting of quasar doublet absorption lines probe smaller redshifts, but should be much more reliable. Unfortunately, the two groups which have been actively studying this topic report different results. Webb and collaborators [18] were the first to report a positive result:

$$\Delta\alpha/\alpha = (-1.9\pm 0.5)\times 10^{-5}, \quad z\sim 1.0\text{–}1.6. \tag{4}$$

Note that this means that α was *smaller* in the past. Recently the same group reports two more (as yet unpublished) positive results [19], $\Delta\alpha/\alpha = (-0.75\pm 0.23)\times 10^{-5}$ for redshifts

*Email address: pedro@astro.up.pt
†Email address: c.j.a.p.martins@damtp.cam.ac.uk
‡Email address: graca@astro.up.pt
§Email address: viana@astro.up.pt

$z \sim 0.6-1.6$ and $\Delta\alpha/\alpha = (-0.74 \pm 0.28) \times 10^{-5}$ for redshifts $z \sim 1.6-2.6$. On the other hand, Varshalovich and collaborators [13] report only a null result:

$$\Delta\alpha/\alpha = (-4.6 \pm 4.3 \pm 1.4) \times 10^{-5}, \quad z \sim 2-4. \tag{5}$$

The first error bar corresponds to the statistical error while the second is the systematic one. This corresponds to the bound

$$|\dot{\alpha}/\alpha| < 1.4 \times 10^{-14} \text{ yr}^{-1} \tag{6}$$

over a timescale of about 10^{10} years. It should be emphasized that the observational techniques used by both groups have significant differences, and it is presently not clear how the two compare when it comes to eliminating possible sources of systematic error.

Finally, a third option is the cosmic microwave background (CMB) [11]. This probes intermediate redshifts, but has the significant advantage that one has (or will soon have) highly accurate data.

The reason why the cosmic microwave background is a good probe of variations of the fine-structure constant is that these alter the ionization history of the universe [11,12]. The dominant effect is a change in the redshift of recombination, due to a shift in the energy levels (and, in particular, the binding energy) of hydrogen. The Thomson scattering cross section is also changed for all particles, being proportional to α^2. A smaller effect (which has so far been neglected) is expected to come from a change in the helium abundance.

As is well known, CMB fluctuations are typically described in terms of spherical harmonics,

$$T(\theta,\phi) = \sum_{lm} a_{lm} Y_{lm}(\theta,\phi), \tag{7}$$

from whose coefficients one defines

$$C_l = \langle |a_{lm}|^2 \rangle. \tag{8}$$

Increasing α increases the redshift of last scattering, which corresponds to a smaller sound horizon. Since the position of the first Doppler peak (which we shall denote as l_{peak}) is inversely proportional to the sound horizon at last scattering, we see that increasing α will produce a larger l_{peak} [12]. This larger redshift of last scattering also has the additional effect of producing a larger early integrated Sachs-Wolfe (ISW) effect, and hence a larger amplitude of the first Doppler peak [11]. Finally, an increase in α decreases the high-l diffusion damping (which is essentially due to the finite thickness of the last-scattering surface), and thus increases the power on very small scales.

The authors of [11] provide an analysis of these effects and conclude that future CMB experiments should be able to provide constraints on a varying α at the recombination epoch (that is, at redshifts $z \sim 1000$) at the level of

$$|\dot{\alpha}/\alpha| < 7 \times 10^{-13} \text{ yr}^{-1}, \tag{9}$$

or equivalently

$$|\alpha^{-1} d\alpha/dz| < 9 \times 10^{-5}, \tag{10}$$

which seems to indicate that these constraints can only become competitive in the near future.

Here we analyze these effects for the BOOMERanG [20,21] and MAXIMA [22,23] data. We briefly review the method and then discuss the results in the next section. We find that these data tend to prefer a value of α that was lower in the past. However, we strongly emphasize that there are interesting and so far unnoticed degeneracies in the physics of the problem which imply that this method of determining the fine-structure constant can only produce strong constraints if other cosmological parameters are independently known. We will comment on this point in Sec. III.

While this paper was being finalized, another report appeared [24], containing an independent analysis of the same data. It should be noticed that there are some significant differences in the two analysis procedures, as well as in the results, which we will point out along the way. In the cases where a direct comparison is possible, our work confirms their results, while in the other cases we provide some physical motivation for the differences.

II. DATA ANALYSIS

We perform a likelihood analysis of the recently released BOOMERanG [20] and MAXIMA [22] data, allowing for the possibility of a time-varying fine-structure constant. The method used follows the procedure described in [25,26]. The angular power spectrum C_l was obtained using a modified CMBFAST algorithm which allows a varying α parameter. We have changed the subroutine RECFAST [27] according to the extensive description given in [11].

We vary the power spectrum normalization C_2 within the 95% limits for the Cosmic Background Explorer (COBE) 4-year data [28]. The space of model parameters spans

$$\Omega_0 = (0.1\text{–}1.0), \tag{11}$$

$$\Omega_b h^2 = (0.01\text{–}0.028), \tag{12}$$

$$H_0 = (50\text{–}80), \tag{13}$$

$$\alpha/\alpha_0 = (0.9\text{–}1.1), \tag{14}$$

and the C_l normalization

$$bias = C_2/C_{2,COBE} = (0.83\text{–}1.16). \tag{15}$$

Note that α_0 is the value of the fine structure constant today. The basic grid of models was obtained considering parameter step sizes of 0.1 for Ω_0; 0.003 for $\Omega_b h^2$; 5 for H_0; 0.01 for α/α_0, and finally 0.01 for the $bias$. In order to compute the maxima and the confidence intervals for the 1-dim marginalized distributions we have increased the grid resolution of each of the model parameters using interpolation procedures.

All our models have $\Omega_{total} = 1$ and no tilt. We point out that this is in agreement [29] with the best-fit model for the $\Omega_{total} = 1$ case for the combined analysis of the BOOMER-

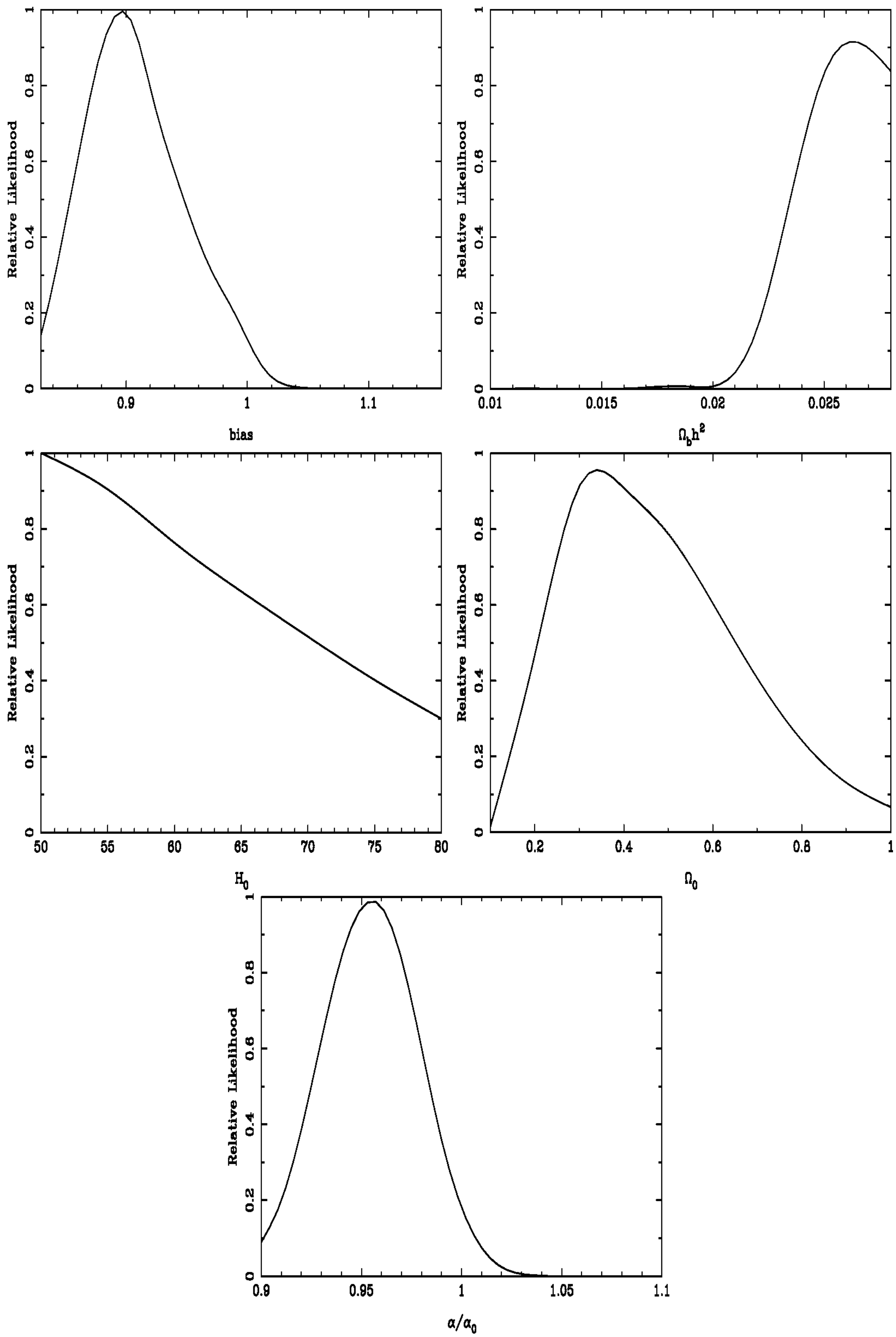

FIG. 1. Marginal distributions for each model parameter for the nominal calibration case.

anG and MAXIMA data. Somewhat surprisingly, the authors of [24] seem to find that the same data prefer tilted models even in the ''standard'' case, that is, without considering a varying fine-structure constant. This will obviously affect their results, as we will discuss below.

We also emphasize that α may or may not have had a different value at the nucleosynthesis epoch, which in particular will affect the value of $\Omega_b h^2$. Since in the present paper we do not treat this effect, the correct approach [8] is to accept the observationally determined value. This is the

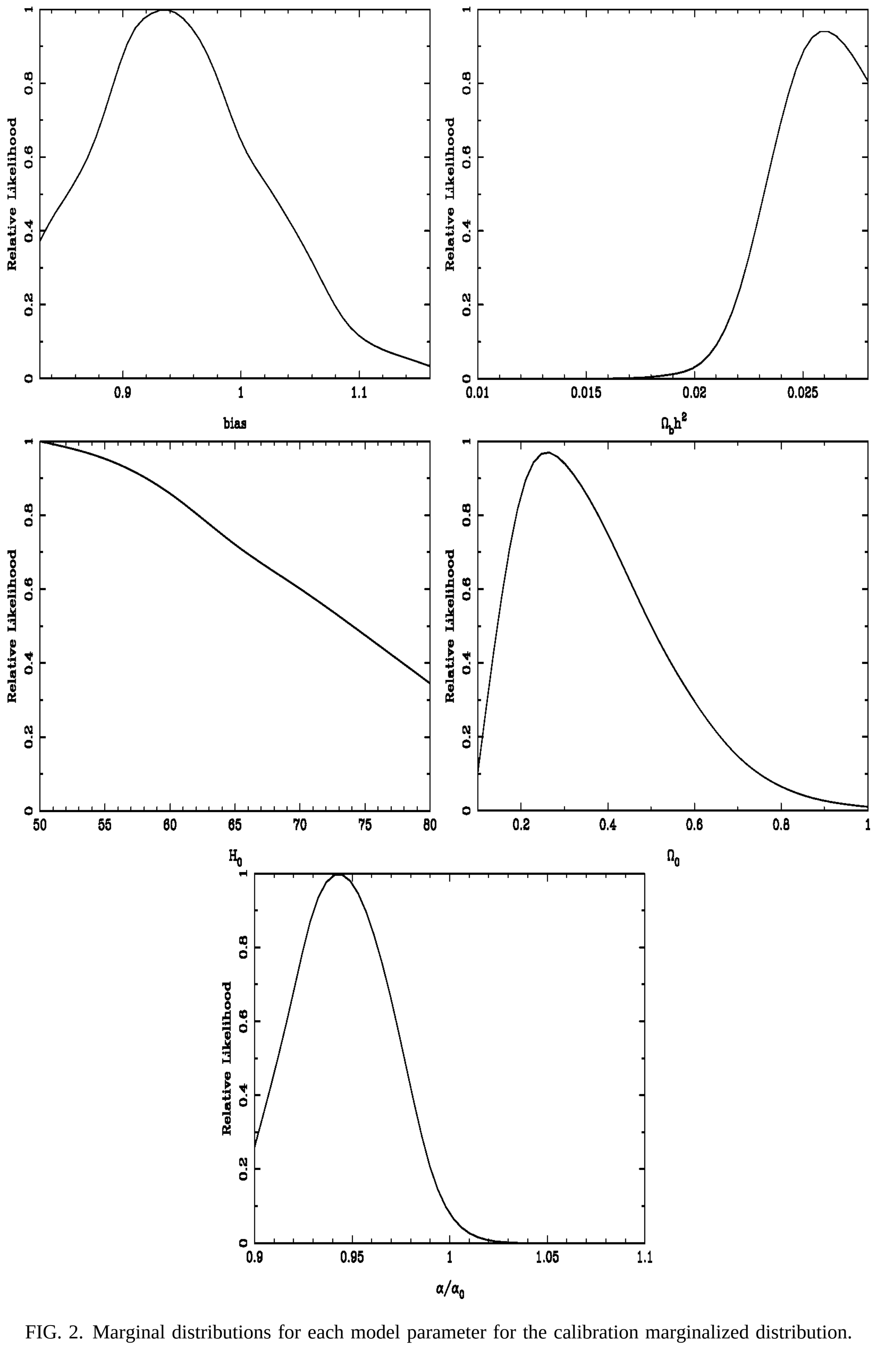

FIG. 2. Marginal distributions for each model parameter for the calibration marginalized distribution.

reason why we ignore excessively high values of $\Omega_b h^2$ which seem to be required by some analyses of the CMB data [21,29].

For each of these C_l spectra we compute the flat band power estimates of the CMB anisotropies obtaining a simulated observation for each data point. These estimates cover the multi-pole range sampled by both BOOMERanG and MAXIMA experiments. The values of Ω_b are obtained as *function* of H_0 in order to satisfy the range for $\Omega_b h^2$ defined above.

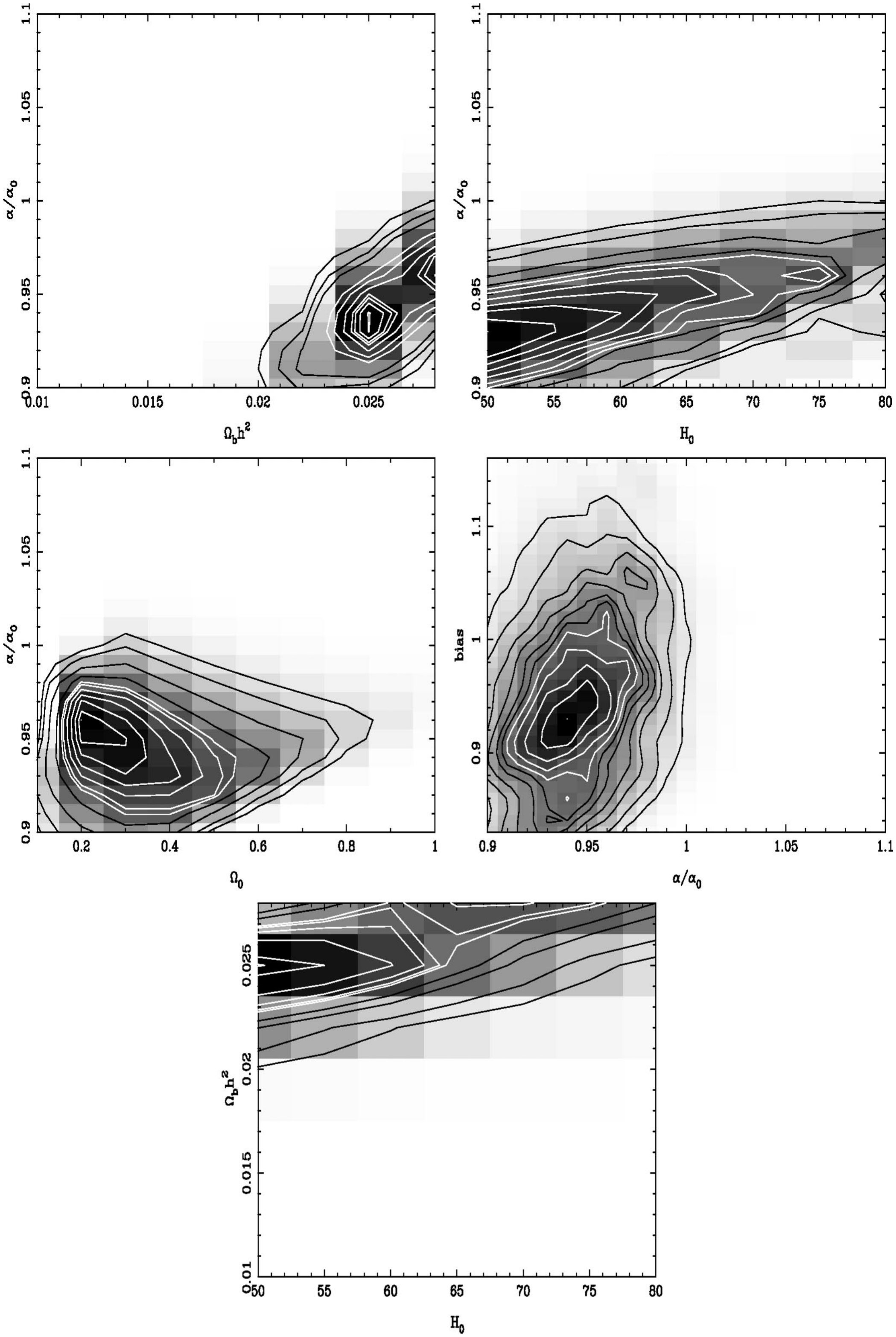

FIG. 3. Confidence contours for the 2-dim distribution obtained after marginalizing over the remaining three parameters (for the calibration marginalized distribution). Contours are at 10,20,30, . . . 90 and 95 percent confidence levels.

A. The full dataset

Interesting conclusions can be drawn by comparing the nominal calibration case for both experiments with the likelihood obtained after marginalizing over the calibration uncertainties of BOOMERanG (20%) and MAXIMA (8%). As mentioned in [30] the fitting to a lower second Doppler peak can be achieved either by increasing the value of $\Omega_b h^2$ or decreasing the value of α/α_0. Note also that there is an additional constraint on α/α_0 coming from the position of the main acoustic peak [12]. We shall comment on the relative importance of the two constraints below.

For the nominal calibration case we obtain a best fit model with

$$H_0=55, \quad \Omega_b h^2=0.025, \quad \Omega_0=0.5, \tag{16}$$

$$\alpha/\alpha_0=0.94, \quad bias=0.87, \quad \chi^2=20.38. \tag{17}$$

In Fig. 1 we plot the marginalized distributions for all the parameters.

For this case the maxima and confidence intervals for the marginalized distributions are as follows (all 1σ): $\alpha/\alpha_0=0.96^{+0.02}_{-0.03}$, $H_0=50^{+16.02}_{-0.00}$, $\Omega_b h^2=0.026^{+0.002}_{-0.001}$, $\Omega_0=0.3^{+0.3}_{-0.1}$; $bias=0.9\pm0.04$.

We then marginalized the 5-dim likelihood function over the calibration uncertainties assuming a Gaussian prior. In this case we obtain a best fit model with

$$H_0=55, \quad \Omega_b h^2=0.025, \quad \Omega_0=0.4; \tag{18}$$

$$\alpha/\alpha_0=0.93, \quad bias=0.91, \quad \chi^2=15.55. \tag{19}$$

In Fig. 2 we plot the marginalized distributions for all the parameters for the distribution marginalized over the calibration errors. Comparing with Fig. 1 we notice that in the case of the marginalized distribution the distributions for Ω_0 and α/α_0 are slightly shifted towards lower values, while those of $\Omega_b h^2$ and H_0 are not significantly affected.

The maxima and confidence intervals for the marginalized distributions are as follows (again, all are 1σ): $\alpha/\alpha_0=0.94^{+0.03}_{-0.02}$, $H_0=50^{+16.62}_{-0.0}$; $\Omega_b h^2=0.026\pm0.002$, $\Omega_0=0.3^{+0.17}_{-0.14}$, $bias=0.94\pm0.07$.

If we consider the best calibration case assuming a uniform prior we get the same best fit set of parameter values as for the calibration marginalized likelihood, apart from the bias (which now has the value $bias=0.84$). The best calibration factor is 1.0 (nominal) for BOOMERanG and 0.92 (ratio with respect to the nominal case) for MAXIMA (this corresponds to $\chi^2=15.73$). This is just telling us that if we keep BOOMERanG at the nominal calibration case and lower the height of the MAXIMA data points we force the normalization of the models to decrease.

If instead we consider the best calibration case assuming a Gaussian prior we get a best fit with a calibration factor of 1.1 for BOOMERanG and 1.0 (nominal) for MAXIMA ($\chi^2=15.75$ before weighting). As should be expected we get a higher best fit value for the model's normalization of $bias=0.92$. Meanwhile for both cases we observe a decrease on the value of Ω_0 from 0.5 to 0.4 and on the value of α/α_0 from 0.94 to 0.93, when compared with the nominal case.

Note that both pushing the BOOMERanG data up or pushing the MAXIMA data down provide for a better overlap of the two data sets. Then the different overall normalizations (in particular the height of the first Doppler peak) account for the different values of the cosmological parameters.

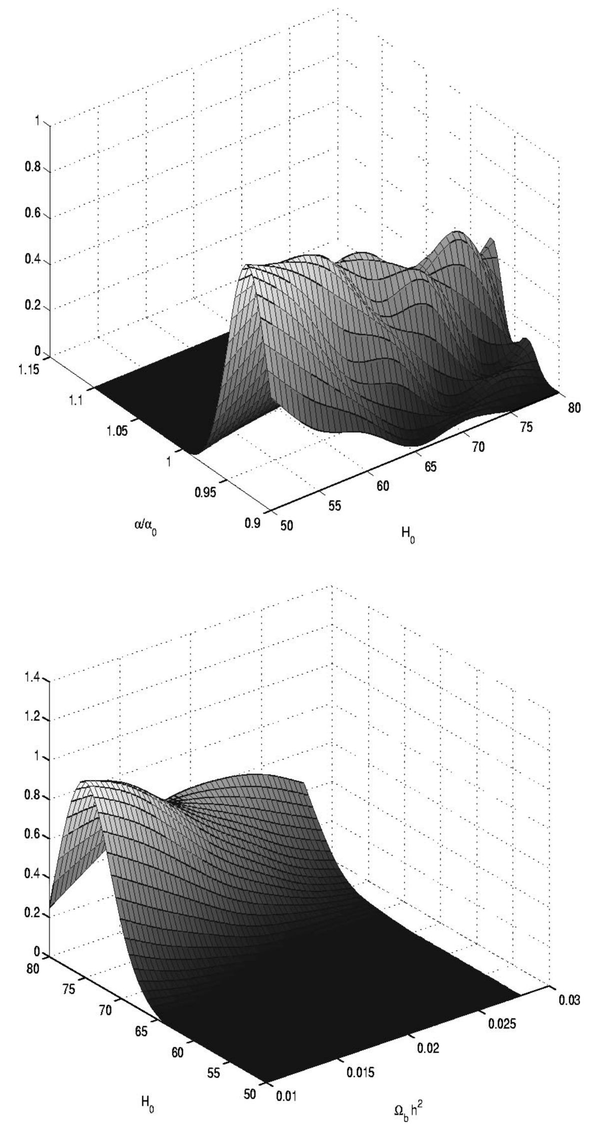

FIG. 4. The likelihood surface for H_0 and α/α_0 (top plot); for $\Omega_b h^2$ and H_0 (bottom plot), for the calibration marginalized distribution.

In Fig. 3 we plot the 2-dim likelihood functions obtained after marginalizing over the remaining three parameters. In Fig. 4 we plot the likelihood surface for H_0 and α/α_0 as well as for $\Omega_b h^2$ and H_0. Similarly, Fig. 5 contains the corresponding likelihoods for the nominal calibration case. This highlights the fact that there are some nontrivial degeneracies in the problem [31]. We shall return to this point below.

It is of interest to investigate the case where no variation of the fine-structure constant is allowed. For that purpose we considered the conditional distribution for $\alpha/\alpha_0=1.0$ to obtain a best fit model with

$$H_0=75, \quad \Omega_b h^2=0.028, \quad \Omega_0=0.3; \tag{20}$$

$$bias=1.0, \quad \chi^2=17.49. \tag{21}$$

In Fig. 6 we plot this distribution marginalized over Ω_0 and the bias. Increasing the value of α seems to force a

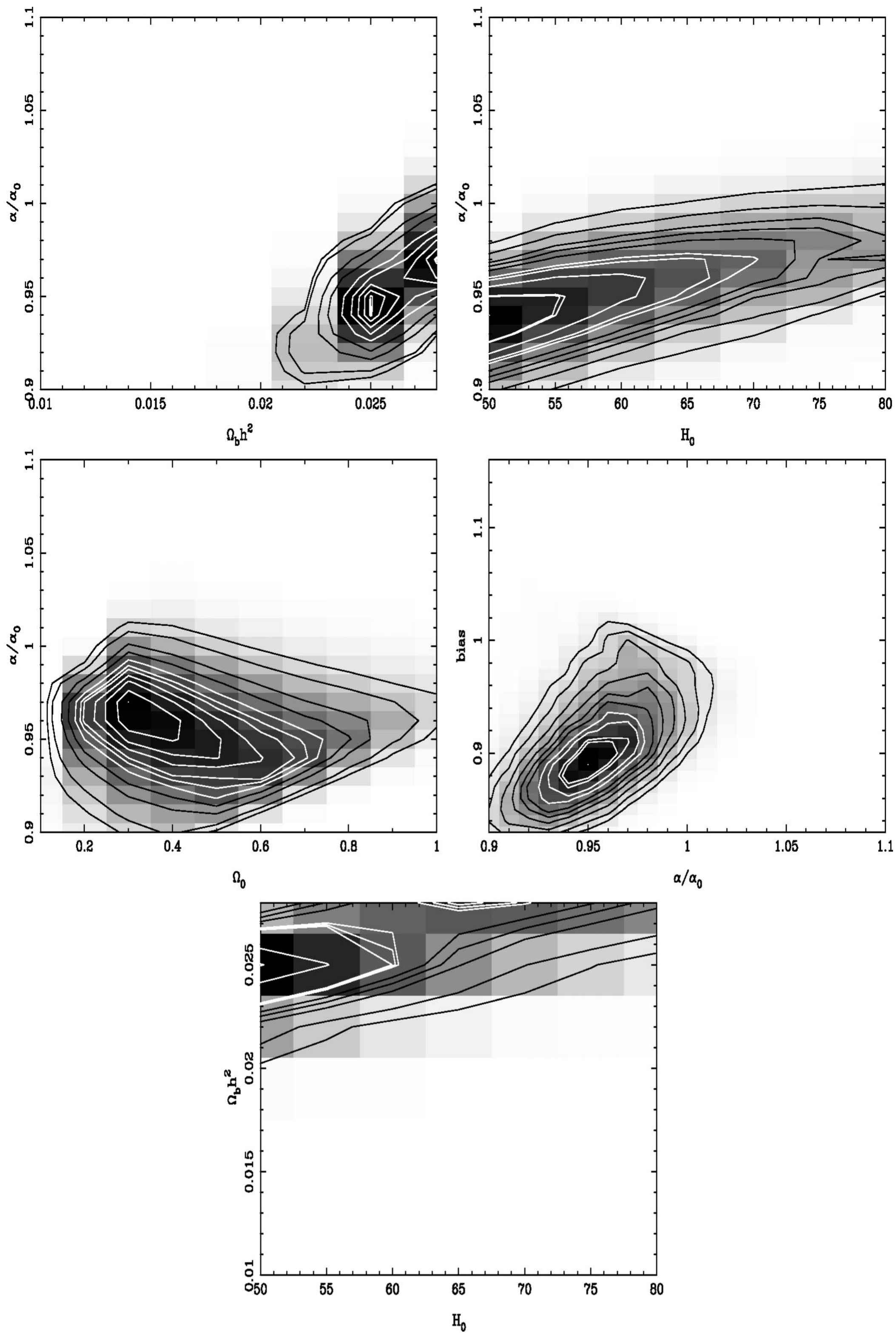

FIG. 5. Confidence contours for the 2-dim distribution obtained after marginalizing over the remaining three parameters (for the calibration nominal case). Contours are at 10,20,30, . . . 90 and 95 percent confidence levels.

higher best fit value of H_0 and of $\Omega_b h^2$ and a lower value of Ω_0 with a best fit COBE normalized model. Again, this is consistent with [29] (which also finds a tilt $n_s = 0.99$, while [24] finds $n_s = 0.92$).

If we instead condition our distribution to a value of $\Omega_b h^2 = 0.019$ we get a best fit model with

$$H_0 = 50, \quad \Omega_0 = 0.3, \quad \alpha/\alpha_0 = 0.9; \tag{22}$$

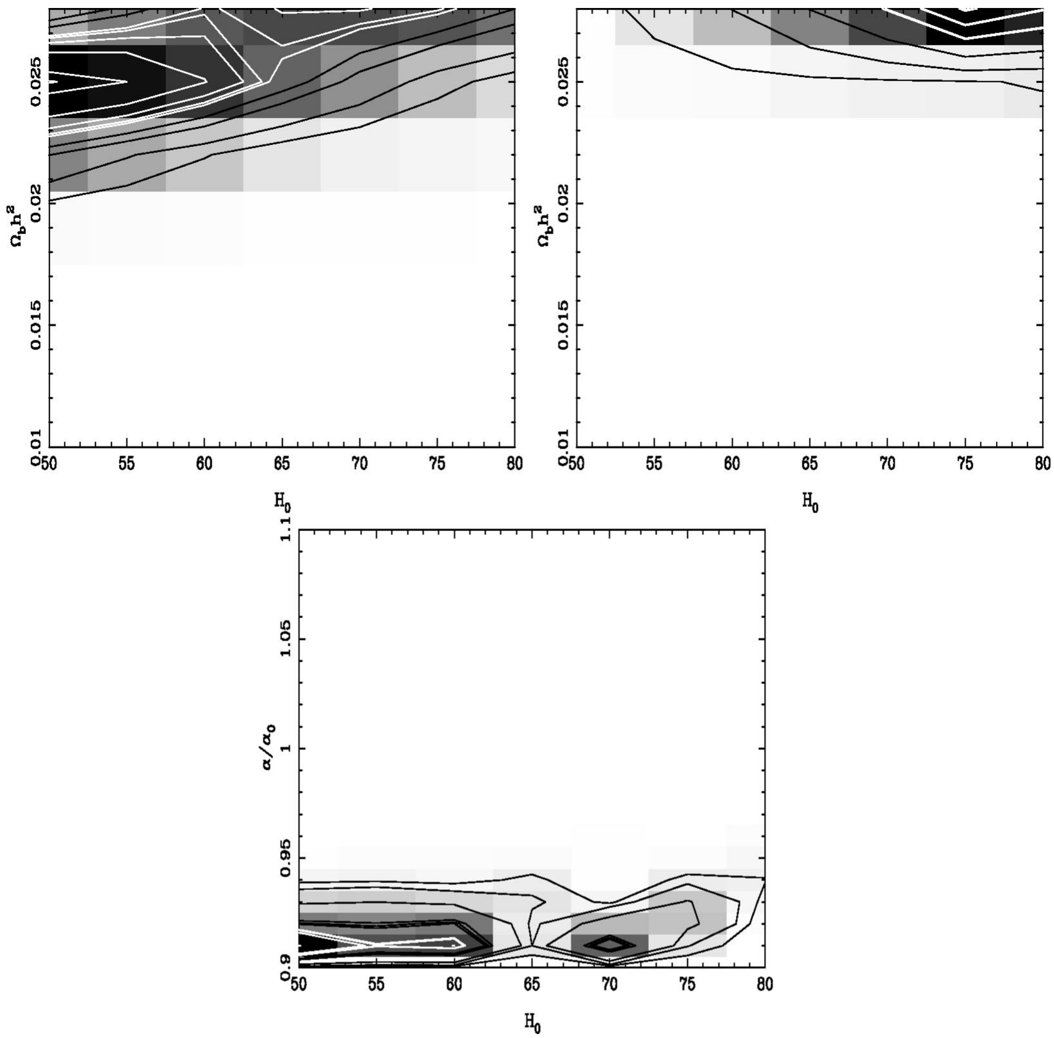

FIG. 6. Confidence contours for the 2-dim distribution of $(H_0,\ \Omega_b h^2)$; marginalized over the remaining parameters (left-hand side plot); conditional distribution for $\alpha/\alpha_0 = 1$ and marginalized over the remaining parameters (right-hand side plot). Bottom plot: Confidence contours for the 2-dim distribution of $(\alpha/\alpha_0,\ H_0)$ conditional to $\Omega_b h^2 = 0.019$ and marginalized over the remaining parameters (for the calibration corrected likelihood). Contours are at 10,20,30, . . . 90 and 95 percent confidence levels.

$$bias = 0.89, \quad \chi^2 = 18.23. \tag{23}$$

This result emphasizes the rather obvious point that reducing the value of $\Omega_b h^2$ requires a lower value of α/α_0 to account for a low second acoustic peak.

Once more, we emphasize that the values of Ω_b are obtained as function of H_0 in order to satisfy the range for $\Omega_b h^2$ defined above. This means that we should expect to observe some correlation when plotting H_0 against $\Omega_b h^2$. This is indeed confirmed by Fig. 3.

Therefore we have so far confirmed the fact that to fit a low second Doppler peak we need a high baryonic content [31,30] and a lower fine-structure constant in the past. However, an important question still remains: what is the weight of the second acoustic peak relative to the main peak in drawing the above conclusions? We recall that in [12] it was shown that the position of the first Doppler peak can by itself provide a constraint on α. Can it happen that the main acoustic peak is still a heavy factor in determining the above best fit parameters?

B. The first Doppler peak

In order to answer this important question, we considered the set of data points sampling the multi-pole region up to $l \sim 400$. Hence this data set consists now of the first 8 BOOMERanG and the first 5 MAXIMA data points with the nominal calibration (BM_{dp}). We then repeat the likelihood analysis for this new data set.

We obtain a best fit model with

$$H_0 = 50, \quad \Omega_b h^2 = 0.019, \quad \Omega_0 = 0.4, \tag{24}$$

$$\alpha/\alpha_0 = 0.9, \quad bias = 0.87, \quad \chi^2 = 14.91. \tag{25}$$

This is rather encouraging, particularly because the best fit value for $\Omega_b h^2$ is precisely the one found by observations. However, the maxima and confidence intervals for the marginalized distributions are as follows (again, all are 1σ): $\alpha/\alpha_0 = 0.97 \pm 0.04$, $H_0 = 71.4^{+6.1}_{-13.5}$; $\Omega_b h^2 = 0.024 \pm 0.003$, $\Omega_0 = 0.4^{+0.33}_{-0.21}$, $bias = 1.0^{+0.05}_{-0.08}$.

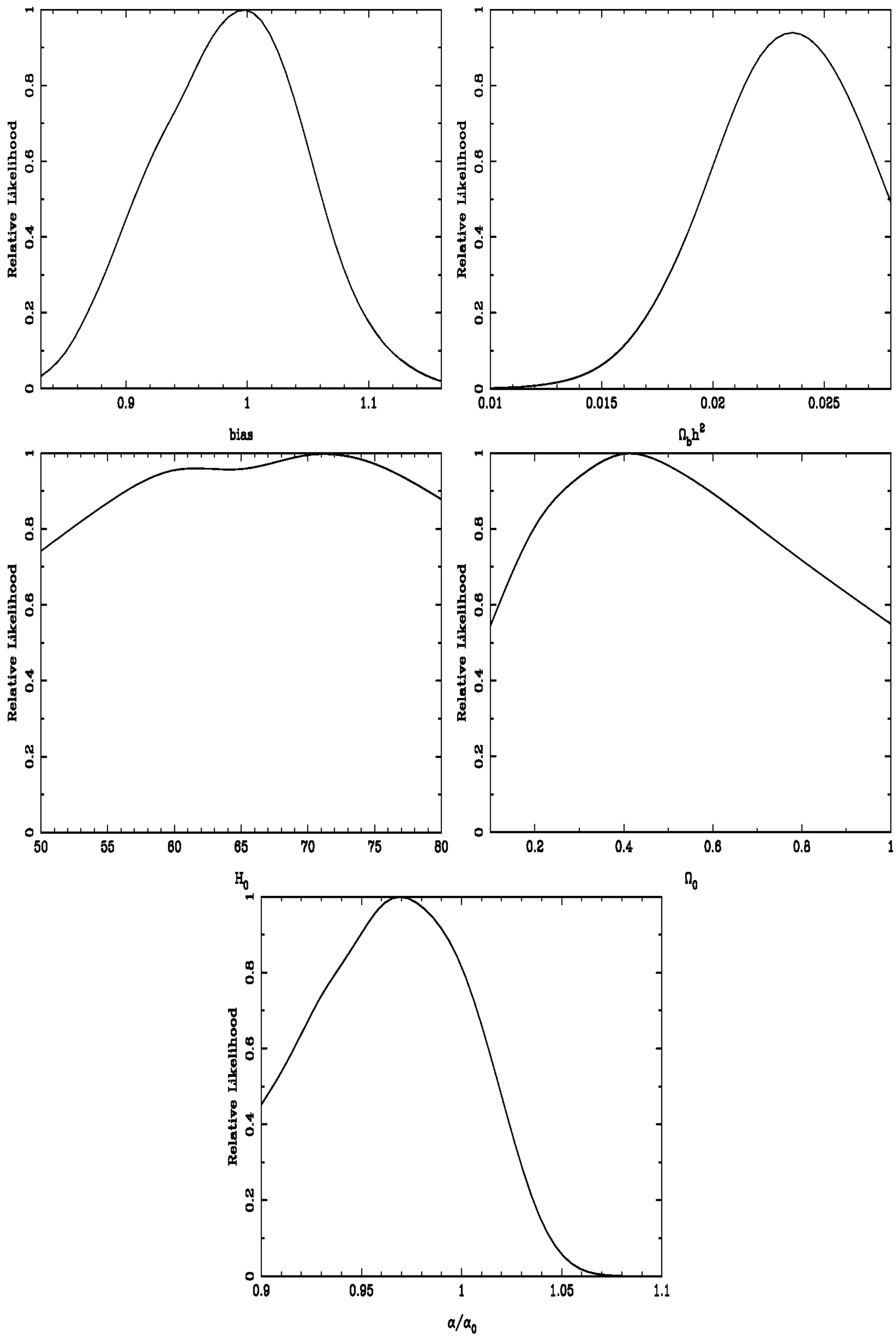

FIG. 7. Marginal distributions for each model parameter for a subsection of data probing the main Doppler peak region (and nominal calibration case) (BM_{dp}).

We conclude that most of the best fit model parameters do not lay within the 1σ range around the maximum of the marginalized distribution for the corresponding parameter. Therefore the 5-dim likelihood must have a narrow peak around this best model with an enlarged surface around the remaining values whose height is not significantly smaller than the absolute peak.

In Fig. 7 we plot the marginalized distributions for all the

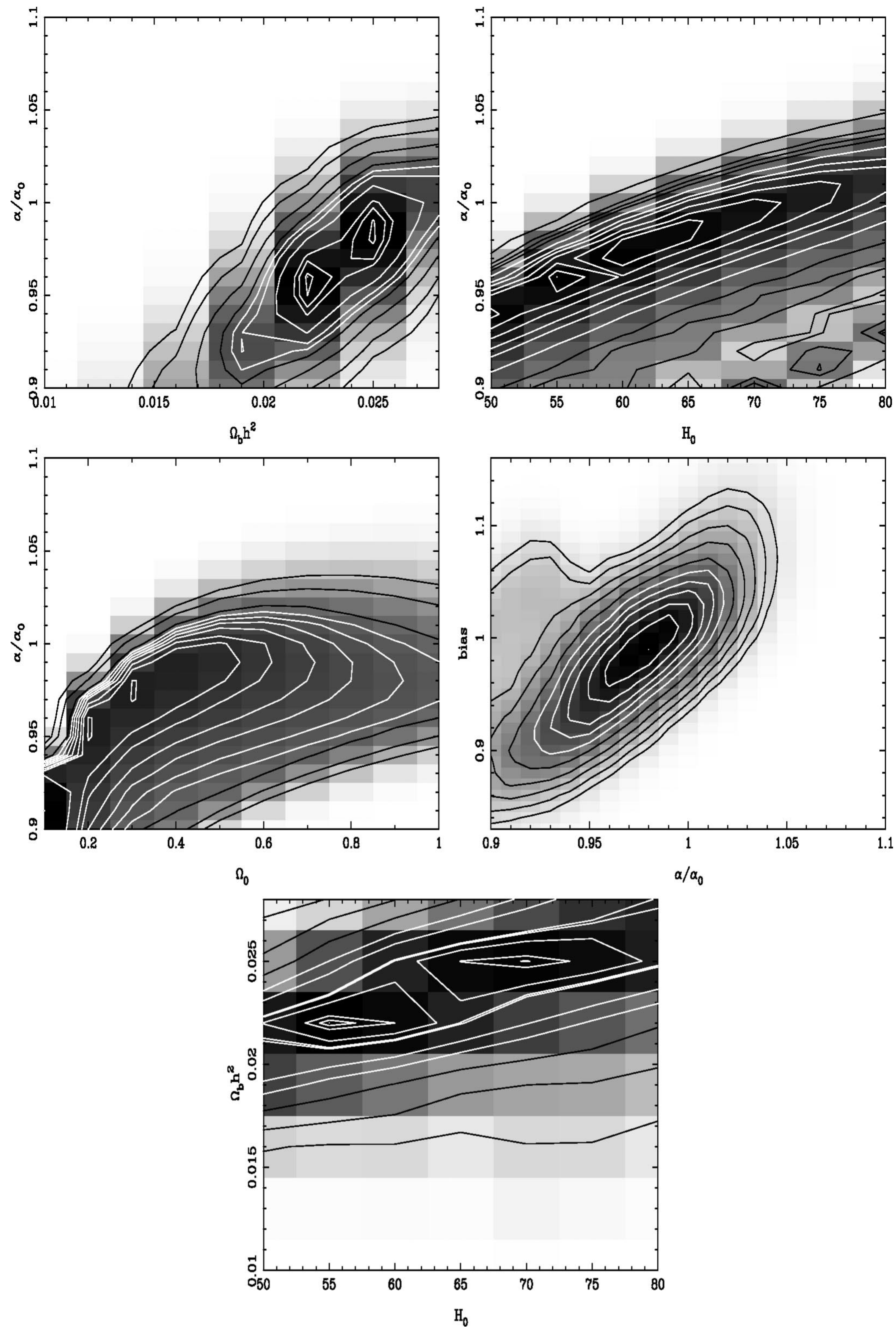

FIG. 8. Confidence contours for the 2-dim distribution obtained after marginalizing over the remaining three parameters for BM_{dp}. Contours are at 10,20,30,$\ldots$90 and 95 percent confidence levels.

parameters, while in Fig. 8 we plot the 2-dim likelihood functions obtained after marginalizing over the remaining three parameters.

Comparing Fig. 7 with Fig. 1, we immediately notice a number of extremely interesting points. First, even though the data set for the first Doppler peak favors a smaller α in the past, there is a non-negligible likelihood for *larger* values as well. The inclusion of information from the second Doppler peak all but eliminates this possibility (compare this with Fig. 4 of [24]). Secondly, the full data set *increases* the

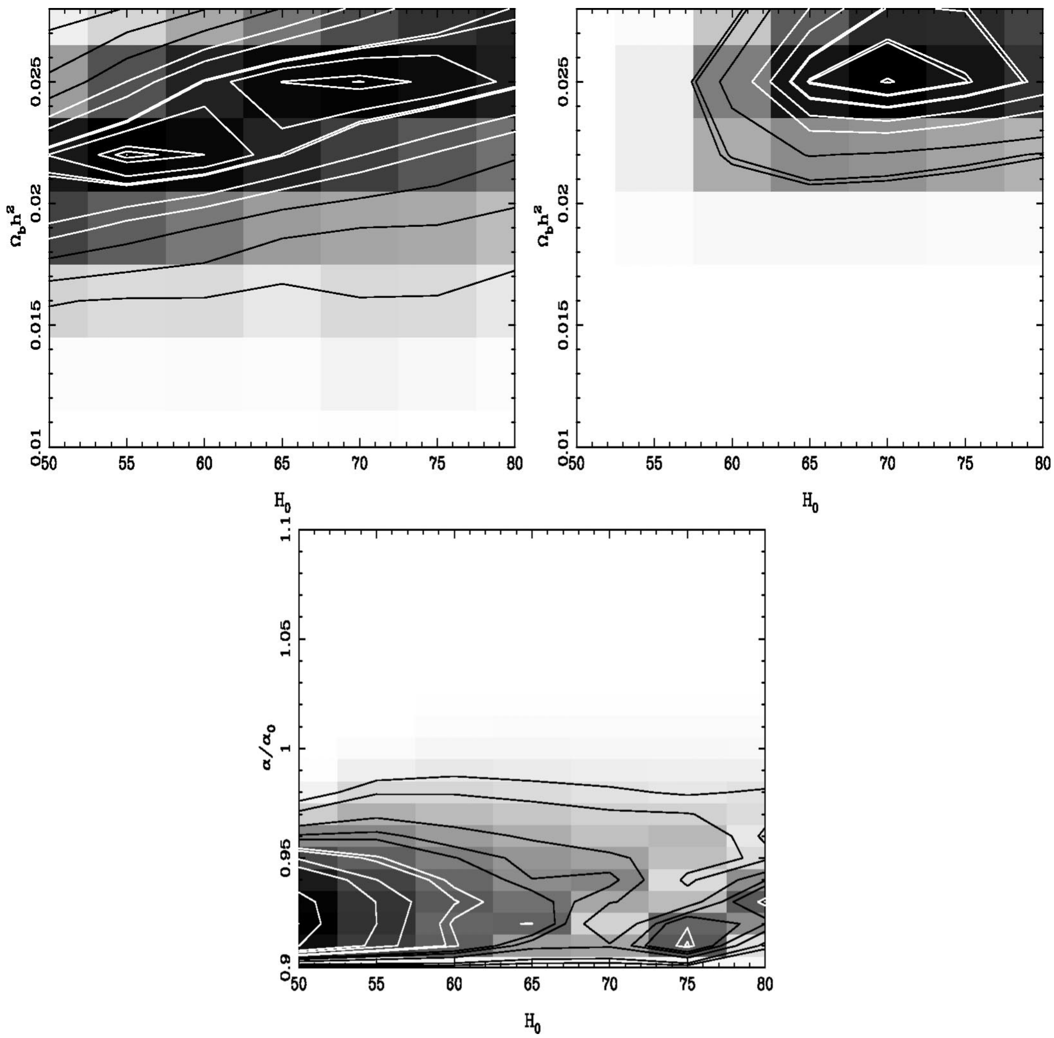

FIG. 9. Confidence contours for the 2-dim distribution of $(H_0,\ \Omega_b h^2)$; marginalized over the remaining parameters (left-hand side plot); conditional distribution for $\alpha/\alpha_0=1$ and marginalized over the remaining parameters (right-hand side plot). Bottom plot: Confidence contours for the 2-dim distribution of $(\alpha/\alpha_0,\ H_0)$ conditional to $\Omega_b h^2=0.019$ and marginalized over the remaining parameters (for BM_{dp}). Contours are at 10,20,30, . . . 90 and 95 percent confidence levels.

preferred values of $\Omega_b h^2$ (or more accurately, decreases the probability for low values). And thirdly, data from the first Doppler peak alone are basically insensitive to H_0 and Ω_0 (recall that all our models have $\Omega_{total}=1$), while the full data set tends to favor low values of H_0 and also narrows the distribution for Ω_0 around a value of $\Omega_0=0.3$ (and most notably reduces the probability of lower values such as $\Omega_0=0.1$ which would be allowed by the reduced data set).

This might explain the differences in the contour plots of the 2-dim distribution of $(\alpha/\alpha_0,\ \Omega_0)$ in Fig. 8 and Fig. 5; the plot in Fig. 8 shows a correlation between $(\alpha/\alpha_0,\ \Omega_0)$ which disappears when including the other Doppler peaks. These 2-dim plots do also indicate correlations between $(\alpha/\alpha_0,\ H_0)$; $(\alpha/\alpha_0,\ \Omega_b h^2)$ and $(\alpha/\alpha_0,\text{bias})$ which do exist in both situations.

Finally, we also consider the case with no variation of the fine-structure constant allowed for the reduced data set. We obtain a best fit model with

$$H_0=75, \quad \Omega_b h^2=0.025, \quad \Omega_0=0.5; \tag{26}$$

$$bias=1.02, \quad \chi^2=15.24. \tag{27}$$

If now we condition our distribution to a value of $\Omega_b h^2=0.019$ we get a best fit model with

$$H_0=50, \quad \Omega_0=0.4, \quad \alpha/\alpha_0=0.9; \tag{28}$$

$$bias=0.87, \quad \chi^2=14.91. \tag{29}$$

In Fig. 9 we plot these conditional distributions marginalized over Ω_0 and the bias.

III. DISCUSSION AND CONCLUSIONS

In this paper we have performed a likelihood analysis of the combined BOOMERanG and MAXIMA data sets, allowing for the possibility of a time-varying fine-structure constant, for which there is further observational evidence elsewhere [18,19]. We have confirmed the intuitively obvious expectation that these data prefer a value of α that was smaller in the past by a few percent.

However, we wish to emphasize that this is not the same as saying that the CMB can readily provide an unambiguous measurement of the fine-structure constant. As we hopefully made clear above, there are some interesting degeneracies in the problem which imply that other cosmological parameters could still fairly easily mimic a varying α. Hence this method of measurement of α is still far from being ''competitive,'' in the sense that statements about α will not be possible until independent accurate determinations of $\Omega_b h^2$ and H_0 (and possibly other parameters) are available.

We have also shown that the main reason behind the preferred lower value of α in the present data set still comes mainly from the data points around the first Doppler peak. The main effect of the high-l data points is to increase the preferred value for $\Omega_b h^2$ and eliminate the possibility of a larger fine-structure constant in the past. A secondary (from this perspective) effect of the small angular scale data is to tighten the constraints on other parameters. Furthermore, we believe that this relative dominance of the low-l measurements will remain even in the post Microwave Anistropy Probe (MAP) era.

ACKNOWLEDGMENTS

We thank Bruce Bassett, Pedro Ferreira, João Magueijo, Anupam Mazumdar, and Paul Shellard for useful discussions and comments. C.M. and G.R. are funded by FCT (Portugal) under ''Programa PRAXIS XXI,'' grant no. PRAXIS XXI/BPD/11769/97 and PRAXIS XXI/BPD/9990/96, respectively. We thank Centro de Astrofísica da Universidade do Porto (CAUP) for the facilities provided. G.R. also thanks the Department of Physics of the University of Oxford for support and hospitality during the progression of this work.

[1] J. Polchinski, *String Theory* (Cambridge University Press, Cambridge, England, 1998).

[2] T. Banks, hep-th/9911067 (1999).

[3] A. Chodos and S. Detweiler, Phys. Rev. D **21**, 2167 (1980); W. J. Marciano, Phys. Rev. Lett. **52**, 489 (1984).

[4] Y. S. Wu and Z. W. Wang, Phys. Rev. Lett. **57**, 1978 (1986).

[5] E. Kiritsis, J. High Energy Phys. **10**, 10 (1999); S. H. S. Alexander, hep-th/9912037 (1999).

[6] J. W. Moffat, Int. J. Mod. Phys. D **2**, 351 (1992); astro-ph/9811390 (1998).

[7] A. Albrecht and J. Magueijo, Phys. Rev. D **59**, 043516 (1999); J. D. Barrow, *ibid.* **59**, 043515 (1999); J. D. Barrow and J. Magueijo, Phys. Lett. B **443**, 104 (1998).

[8] P. P. Avelino and C. J. A. P. Martins, Phys. Lett. B **459**, 468 (1999).

[9] P. P. Avelino and C. J. A. P. Martins, Phys. Rev. Lett. **85**, 1370 (2000).

[10] J. D. Bekenstein, Phys. Rev. D **25**, 1527 (1982).

[11] S. Hannestad, Phys. Rev. D **60**, 023515 (1999); M. Kaplinghat, R. J. Scherrer, and M. S. Turner, *ibid.* **60**, 023516 (1999).

[12] P. P. Avelino, C. J. A. P. Martins, and G. Rocha, Phys. Lett. B **483**, 210 (2000).

[13] D. A. Varshalovich, A. Y. Potekhin, and A. V. Ivanchik, physics/0004062 (2000).

[14] J. D. Prestage, R. L. Tjoelker, and L. Maleki, Phys. Rev. Lett. **74**, 3511 (1995).

[15] T. Damour and F. Dyson, Nucl. Phys. **B480**, 37 (1996).

[16] P. D. Sisterna and H. Vicetich, Phys. Rev. D **41**, 1034 (1990).

[17] L. Bergstrom, S. Iguri, and H. Rubinstein, Phys. Rev. D **60**, 045005 (1999).

[18] J. K. Webb *et al.*, Phys. Rev. Lett. **82**, 884 (1999).

[19] J. K. Webb *et al.*, seminar at IoA, Cambridge, 2000.

[20] P. de Bernardis *et al.*, Nature (London) **404**, 939 (2000).

[21] A. E. Lange *et al.*, astro-ph/0005004 (2000).

[22] S. Hanany *et al.*, astro-ph/0005123 (2000).

[23] A. Balbi *et al.*, astro-ph/0005124 (2000).

[24] R. A. Battye, R. Crittenden, and J. Weller, astro-ph/0008265 (2000).

[25] S. Hancock, G. Rocha, A. N. Lasenby, and C. M. Gutierrez, Mon. Not. R. Astron. Soc. **294L**, 1 (1998).

[26] G. Rocha, in *Dark Matter in Astrophysics and Particle Physics* 1998, edited by H. V. Klapdor-Kleingrothaus and L. Baudis (Institute of Physics, Bristol, 1999).

[27] S. Seager, D. Sasselov, and D. Scott, Astrophys. J. Lett. **523**, L1 (1999); astro-ph/9912182 (1999).

[28] C. L. Bennett *et al.*, Astrophys. J. Lett. **464**, L1 (1996).

[29] A. Jaffe *et al.*, astro-ph/0007333 (2000).

[30] M. White, D. Scott, and E. Pierpaoli, astro-ph/0004385 (2000).

[31] W. Hu and N. Sugiyama, Astrophys. J. **444**, 489 (1995); Phys. Rev. D **51**, 2599 (1995).